Diagnosis of Skin Cancer Using Image Texture Analysis

Dalia N. Abdul-wadood, Dr. Loay E. George, Dr. Nabeel A. Rasheed

Abstract —In this paper a system that determines whether a given skin lesion microscopic image is malignant or benign is introduced; in case of malignancy, the system can specify its type; whether it is squamous cell carcinoma or basal cell carcinoma (the two leading skin cancer types). In this work 80 images of skin tissue belong to the normal, benign and the two types of skin cancer (squamous and basal) have been collected and used us training and testing material. The samples were obtained from the Pathology Division/ Department of the Central Public Health Laboratory/ Ministry of Health as well as from other different Iraqi hospital pathology departments.
The proposed system passes through two main phases: training phase and testing phase. For both of them, the system implies three main stages (i.e., preprocessing, partitioning & feature extraction). The preprocessing stage implies some image processing operations (including: enhancement, allocation of white smooth areas and quantization). The next stage is partitioning the skin tissue image into overlapping blocks (sub-samples). In the third stage a set of discriminating texture based features is extracted from each sub-sample to build the features vector. The minimum distance (similarity) was used to make the recognition decisions.
Many types of textural features have been tested to evaluate their discrimination ability for successful classification of skin tissues. In the training phase, the system was trained using a set of 50 skin tissue images, the textural features extracted from training samples were analyzed and their discrimination powers were evaluated in order to get a list of the most suitable features for auto recognition task. In case of using co-occurrence features the best attained recognition rates reached (%87.68) for allocation accuracy rate, and (%92.5) for diagnosis accuracy rate, while when using combinations of different textural types of features the best attained recognition rates reached to (%89.92) for allocation accuracy rate, and (%93.75) for diagnosis accuracy rate.

Key Words: Medical image classification, Cancer detection, medical image analysis, textural analysis, minimum distance classifier.

1 Introduction

Since five decades ago, cancer had been one of the biggest threats to human life; it is expected to become the leading cause of death over the next few decades. Based on statistics from the World Health Organization (WHO), cancer accounted for 13% of all deaths in the world in 2004. Deaths caused by cancer are expected to increase progressively in the future, with an estimated 12 million people dying of the disease in 2030. Of all the known cancers, those of the skin are of major concern in both developed and developing countries over the past 40 years with an incidence that has been increased in recent years. However, the survival rate is quite high if the cancer is detected in its early stages. Hence, the early detection of malignant skin lesions is critical to preventing death [1]. The major causes of skin cancers are: (i) the depletion of ozone layer caused by air pollution and (ii) the excessive exposure of the skin to ultraviolet (UV) radiation from the sun and other sources (such as tanning booths). UV radiation is capable of damaging skin cells and causing the cells to grow in erratic fashion [2]. There are three common types of skin cancer, basal cell carcinoma, squamous cell carcinoma and melanoma. Some other types of cancer are exit, but they considered more rare forms of skin cancer. The two most common forms of skin cancer are basal cell carcinoma and squamous cell carcinoma. Together, these two are also referred to as non-melanoma skin cancer [3].

There are different ways to evaluate and diagnose skin cancers. Most dermatologists rely on biopsy of the lesion for definitive diagnosis. Pathologists then examine histological sections derived from such biopsies to make a final definitive diagnosis; this depends on assessing cell morphology and architectural distribution of the cancerous cells [4]. In some instances the definite histopathological diagnosis of malignancy is difficult; this is particularly so when there is overlap in morphological features between some malignant and benign lesions [5]. Computer-based automatic diagnosis system seems to be an important tool for such difficult cases. In other words, it is considered to be a "double reading" system, in addition to pathological interpretation, where pathologists can take into consideration the information provided by the computer before making their final decision [6]. Computer is not more intelligent than human brain, but it may be capable of extracting some information, such as texture features, that may not be readily perceived by human eyes [7].

- *Dalia N. Abdul-wadood is currently pursuing masters degree program in Computer Science in Baghdad University, Iraq. E-mail: dalia.nabeel@yahoo.com*
- *Dr. Loay E. George is currently Computer department chief in college of Science in Baghdad University, Iraq. E-mail: loayedwar57@yahoo.com*

2 Methodology

This section presents the design considerations and implementation steps of the introduced system for skin cancer tissue diagnosis from optical microscope images. The proposed system is based on utilizing the textural features and the traditional minimum distance classification (MDC) method. Figure 1 shows the main components of the proposed system.

2.1 Skin Tissues Image Acquisition

The unavailability of reference database of skin cancer images had obliged us to look for stained sections (glass

slides) of skin cancer biopsy cases from the central medical laboratory/ ministry of health and different Iraqi hospital pathology departments. Taking images from these sections, was conducted through using microscope-attached digital camera, it was performed with the help of an experienced pathologist. The pathologist was required to pin-point the areas of interest in histological sections see figure2.In this work, 80 samples of skin tissue are collected. The taken samples include both the normal and abnormal skin tissue. The samples images have bitmap (BMP) format with color depth 24 bit/pixel; and the size of each image is (1280x1024) pixels.

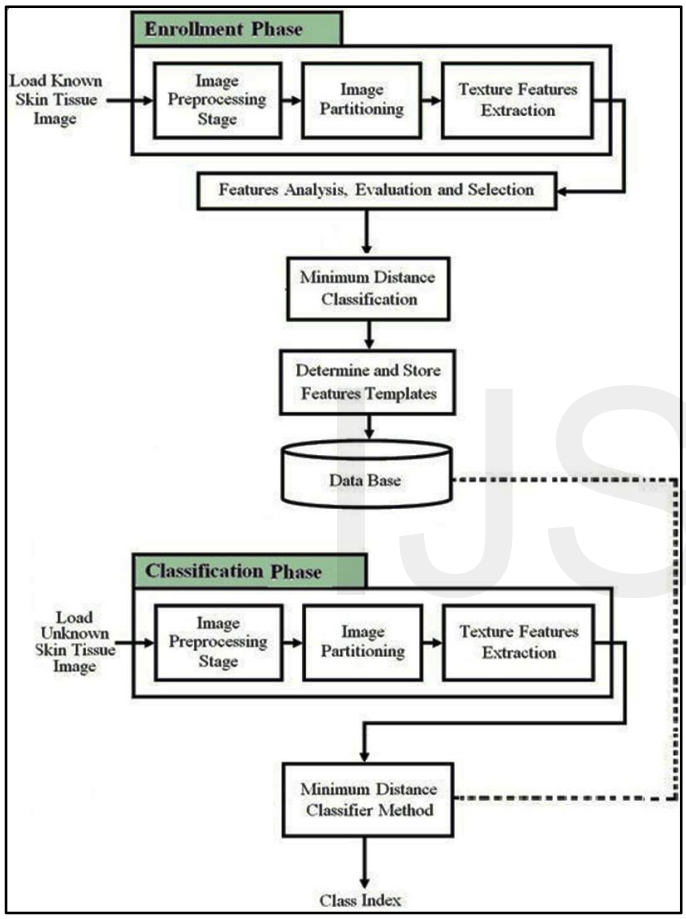

Fig. 1. General Diagram of the Proposed System

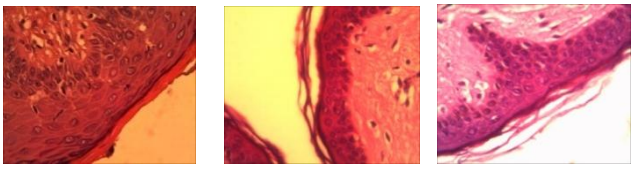

Fig. 2. The Microscopic Image of the Stained Sections (Glass Slides) from Skin Cancer Biopsy Cases

2.2 Pre-Processing Stage

The first stage in any recognition system is pre-processing; in this stage, a set of image processing operations are performed in order to get the best results.

2.2.1 Color Decomposition

When the image file is loaded, then the loaded bitmap pixels (RGB) data are fill-in the Red(), Green(), and Blue() arrays; each array is assigned for one primary color. Along with Red, Green, and Blue color values of the bitmap image, the corresponding gray color values are computed using

$$Gry = 0.3\,R + 0.59\,G + 0.11\,B \quad (1)$$

2.2.2 Contrast Enhancement

Contrast enhancement is very important step because the given image may have color intensities constrained to be within very narrow range or there the opposite situation exist; that is there is artificial local variation in color intensities. The applied contrast stretching comprises of several steps;

Step1: calculate the mean and standard deviation and consequently the min and max parameters values by

$$\mu = \frac{1}{WH}\sum_{y=0}^{H-1}\sum_{x=0}^{W-1}(Img(x,y)) \quad (2)$$

$$\sigma = \frac{1}{WH}\sqrt{\sum_{y=0}^{H-1}\sum_{x=0}^{W-1}(Img(x,y)-\mu)^2} \quad (3)$$

$$min = \mu - \alpha\sigma \quad (4)$$

$$max = \mu + \alpha\sigma \quad (5)$$

Where, $\sum$ is the summation symbol, Img() are the image elements values, and (W,H) are image width and height, respectively.

Step2: linear stretching is applied; it shifts the low color values that are less than the determined (min) value toward 0, and the high level values higher than (max) value is shifted toward 255. The color level values lay between min and max values are linearly mapped by

$$N(x,y) = \left(\frac{255}{max-min}\right)(Img(x,y) - min) \quad (6)$$

As a result, the range of color levels is stretched to the full range (0-255), see figure (3).

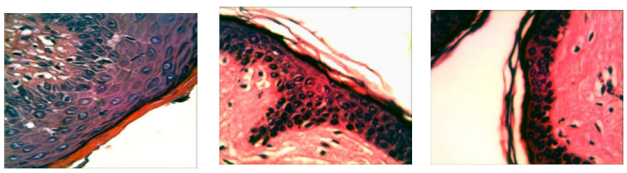

Fig. 3. The Result of Color Stretching on the Images Shown in Fig. 2.

2.2.3 Determination of Small Artificial White Gaps

In tissue section of skin cancers, there are small white artificial gaps arising from mechanical disruption of the tissue by the microtome knife (cutting machine), see figure (4). These white gaps must not be included within the region of interest. Otherwise, they would affect the outcome of the classification. To do the task of white gaps removal, at first the mean filter is applied on the image. The mean filter smoothen the image data and eliminates the noise. This filter performs spatial filtering on each individual pixel by using a square window surrounding each pixel. The mean filter is obtained through computing the sum of all pixels in the filter window and then dividing the sum by the number of pixels in the filter window:

$$\text{Mean}(x,y) = \frac{1}{(L+1)^2}\sum_{-(L-1)/2}^{(L-1)/2}\ \sum_{-(L-1)/2}^{(L-1)/2} \text{Img}(x+i, y+j) \qquad (7)$$

Where, Mean () is the mean filter value, L is the length of the square window. In this step the mean filter is applied on the gray color component only, and L is set 3. In the next step after mean filtering, the standard deviation for the region around each pixel is determined using equation (3). If the mean value of a pixel is large and its standard deviation is small then the pixel is regarded as a white gap pixel. The reason for adopting this criterion (i.e., "large mean value and low standard deviation ") is the fact that these gaps appear in form of white patches (rather than being individual separated white pixels) so all neighboring pixels have values close to each other.

(a) (b)

Fig. 4. (a) Small White Artificial Gaps Lay Inside the Region of Interest. (b) The Detected Small White Gaps in the Image.

2.2.4 Extraction the Region of Interest

Because of the irregularity of the outlines of the tumor components and its different growth patterns under the microscope, automatic segmentation of different structures was difficult. So, one should make a mask to the region of interest in the tissue sections under pathologist supervision; who defines such regions. As a result, regions of interest (ROI) are extracted and everything else is eliminated (i.e., it is set to zero in the mask) as shown in figure (5).

Fig. 5. The Selected Region of Interest in the Image Shown in fig. 4 it is Colored as Red Area, Everything Else is Eliminated

2.2.5 Uniform Quantization

The main drawback in using the Co-occurrence and Run Length matrices is the large memory requirement for storing these matrices; this causes high computational complexity. In such case, the existing granular behavior in adjacent pixel values may cause a loss in the power of discrimination of the extracted features. Scalar quantization process overcomes this problem by removing some of the information details through mapping a group of close data values to single a value by

$$Q = \text{round}\left(\frac{G_{levels}-1}{\max-\min}(G-\min)\right) \qquad (8)$$

This equation is used to map each pixel value from the range (0 to 255) to a new (0 to QLevel-1); where Glevels represents the number of quantized levels. The four color channels in the image will be quantized.

2.3 Image Partitioning

To describe the local features variations, the image is divided into overlapped blocks. Each block has size (LxL), where L is the block length. The value of overlapping length is described in terms of the ratio of block length. (see figure 6).

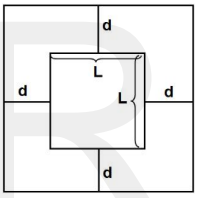

Fig. 6. Illustration of the Overlapped Block, where L is the Block Length and d is the overlapping length

In enrollment phase only the blocks inside the ROI are taken, so the number of ROI pixels in the block is calculated. If the number of non ROI pixels in the block is more than ROI pixels then the block is excluded. Only the blocks have large number of ROI pixels will be taken (see figure 7).

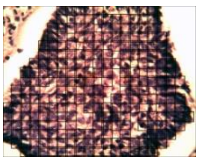

Fig. 7. Representation of Overlapped Blocks Lay within the ROI (During the Enrollment Phase)

2.4 Texture Feature Extraction

After passing through the preprocessing steps, the feature extraction stage begins. When the input data is too large to be processed and suspected to be redundant (i.e., much data, but not much information), then the input data could be transformed into a reduced representation set of features

(also named features vector). Many texture analysis methods have been introduced over the past few decades; two of such methods were used in this work; they are the co-occurrence matrix feature and the run length features. Also, two new sets of features have been developed in this work; they are the global and local roughness measures as additional discriminating tissues features.

A. CO-OCCURRENCE MATRIX (GLCM)

It is a matrix of frequencies at which the values of two of pixels, separated by a certain distance, occur in the image, the content of the GLCM matrix depend on the scan direction and the distance relationship between pixels. Thirteen of Haralick features have been used in this work; they are: Energy (Angular second momentum), Contrast, Correlation, Variance (sum of squares), Inverse difference moment, Entropy, Sum average, Sum Entropy, Sum Variance, Difference variance, Difference Entropy, Information measures of correlation1, Information measures of correlation2.

B. RUN LENGTH MATRIX

It captures the coarseness of a texture in specified directions. A run is a string of consecutive pixels which have the same intensity along a specific linear orientation. Fine textures tend to contain more short runs with similar intensities, while coarse textures have more long runs with significantly different intensities. From each run length matrix, eleven statistical texture features can be computed they are: Short Run Emphasis, Long Run Emphasis, Gray Level Distribution, Run Length Distribution, Run Percentage, Low Gray-level Run Emphasis, High Gray-level Run Emphasis, Short Run Low Gray-level Emphasis, Short Run High Gray-level Emphasis, Long Run Gray-level Emphasis, Long Run High Gray-level Emphasis.

C. GLOBAL ROUGHNESS FEATURES

Roughness is another measure of the texture. The 2D image intensity can be imagined as a surface, such that image intensity at any point can be considered as the elevation at the corresponding point. Roughness is quantified by the vertical deviations of a real surface from its ideal form. If these deviations are large, the surface is considered rough; if they are small the surface is smooth. Roughness is typically considered to be the indication for the degree of existing high frequency (i.e., short wavelength) component of the measured surface. The implemented roughness sub module has two stages, the first one aims to determine the deflections (i.e., residue) of pixels values of the original image, from the corresponding smooth values which belong to the image after applying smoothing. The smoothing task is performed using mean filter. The residue values are considered as the roughness values in the image. The roughness indicator is determined as:

$$R_c(x,y) = C(x,y) - mean_c(x,y) \quad (9)$$

Where, meanc(x,y) is a value of color in the smooth image, C(x,y) is a value of color in original image. The roughness moments are determined using the following:

$$Mom_n = \sum_{i=0}^{clevel} (i - mean_c)^n * His(i) \quad (10)$$

Where, n is the moment order and His(i) is the roughness histogram.

D. LOCAL ROUGHNESS FEATURES

This set of contrast features depends on the local variations in the pixels' values relative to their local position in the quantized image. The differences between each pixel value and the pixels surrounding it considered as local roughness indicators. After the local pixels differences are computed for each pixel, the lowest and largest of these differences' values are determined and each is put in a 2D-matrix (i.e., min & max). Then, the image array and the min-max difference matrices are used to determine the local roughness matrix, Rough(). The element Rough(i,j) reflects the repetition number of roughness value (j) with intensity (i). Finally, after the determination of frequency of occurrence for each possible roughness values, the probability is calculated, which in turn is used to calculate the roughness features values using a set of equations similar to those used with run length matrices.

2.5 FEATURES ANALYSIS AND EVALUATION

This task is important to evaluate the discrimination ability of the adopted features for doing successful classification. This stage is required, exclusively, during the enrollment phase. Not all the adopted features can be guaranteed to have acceptable discrimination capability, so a set of analysis tests should be conducted to determine the scattering ratio of each feature in the feature space. Also, the best combinations of discriminating features that leads to highest classification rate should found. The number of used features must be as small as possible, and they should lead to best classification rate. The procedure followed to perform feature analysis task consists of the following steps:

For each set of samples belong to certain class determine the mean $\{\mu_{ij} | i \in [1, NoFeatures], j \in [1, NoClasses]\}$ and the corresponding standard deviation {ij}.

Test each sample value individually, and discard from the list of samples each feature value (fijk) doesn't satisfy the condition: $|f_{ijk} - \mu_{ij}| < 3\sigma_{ij}$. In case of features discarding, repeat steps 1 and 2 till no feature is discarded or 20% of the overall features (belong to certain class and features type) are discarded.

From the remaining list of values determine the mean and standard deviation for the tested feature and for each class separately.

For each class, determine the within-class scattering ratio for each feature individually:

$$Sw(i,j) = \frac{\sigma_{ij}}{\mu_{ij}} \quad (11)$$

If the values of Sw(i,j) for certain feature (i) is mostly low over all classes then the feature is listed as nominated feature according to within scatter test.

For the considered nominated features the between scatter ratio {SB(i)} is determined,

$$S_B(i) = \frac{\sum_{j=1}^{NoClasses} \sigma_{ij}}{\frac{1}{n} \sum_{j=1}^{NoClasses-1} \sum_{k=j+1}^{NoClasses} |\mu_{ij} - \mu_{ik}|} \quad (12)$$

Where,

$$n = \frac{1}{2}(NoClasses + 1)(NoClasses + 2) \quad (13)$$

For each feature, if its SB ratio is low (<0.5) then the feature is considered suitable to be used for classification purpose.

From the considered successful set of features, find the best combination of features that lead to highest classification rate. The classification rate is determined using:

$$R = \frac{\text{No.of Successfull Hits}}{\text{Total No.of Classification Tests}} \quad (14)$$

In this work normalized Euclidean distance measures have been used to determine the similarity degree between the feature vectors, extracted from the tested samples, with the template feature vectors (mean values and the associated standard deviation), each representing certain class:

$$D(T_i, S_j) = \sum_k \frac{|T(i).f(k) - S(j).f(k)|}{T(i).\sigma(k)} \quad (15)$$

Where, T(i).f(k) is the template value of kth feature belong to ith class. S(j).f(k) is the value of kth feature extracted from jth sample.

In order to improve the discrimination ability we can calculate more than one template vector representing each class, this step is useful to compensate the large textural variability that appear in the images samples taken for each class. The degree of noticed variability let us recognize that the use of one template may not be enough to represent all of them in efficient way. After many conducted tests we have found that the use of two templates is required to attain good classification performance; in other words, we found that the assumption of considering each class consists of two sub-classes is suitable.

The applied calculation for the three templates consists of the following steps:

For each feature (j) belongs to certain class (i) determine the mean and standard deviation values; and consider the mean value as the first initial template value T(1,I,j).

From the first template value and standard deviation of each feature determine the initial values of the second and third templates according to the following equations:

$$T(2, i, j) = T(1, i, j) + \alpha\, \sigma_{ij} \quad (16)$$

$$T(3, i, j) = T(1, i, j) - \alpha\, \sigma_{ij} \quad (17)$$

Where, (i) is the class number, (j) is the feature number, and α is a predefined parameter (its value doesn't exceed 1).

Find which sample of each class (from training set) belong to each template by applying Euclidean distance measures; where the smallest difference from a template means that the tested sample belong to the sub class of that template.

From the samples distributes among classes the mean and standard deviation to each template representing the sub class.

As final step the parameters of the best combinations of discriminating features that leads to highest classification rate are stored in a dedicated database. The stored parameters are the mean values and the associated standard deviation for each template representing certain sub-class.

2.6 Recognition Based on Minimum Distance Criteria

In matching stage the templates vectors, which are saved in the database (i.e., the outcomes of the enrollment phase for all classes) are loaded, and then their similarity degree are computed with the feature vector extracted from the samples of tested image. The difference (D) is computed between each feature vector belong to the tested samples and each template features vector using the normalized Euclidean distance measure. Here, in this step only the features belong to best found combination of features are used. By combining the differences of the best combination of discriminating features (Di) the recognition of the sample with the best similar class is done by selecting the smallest value of (Di):

$$D_i(S_j) = \sum_{k=1}^{Nk} D(S_{jk}, T_{ik}) \quad (18)$$

Where, Sjk is the value of kth feature belong to jth sample and Tik is the template value of kth feature belong to ith class.

3. Experimental Results

In this work, 80 samples of skin tissue are collected from the central medical laboratory/ ministry of health and different Iraqi hospital pathology departments. The taken samples include both the normal and abnormal skin tissue (benign tumor and two types of skin cancer (i.e. basal cell carcinoma, squamous cell carcinoma). Table (1) presents the number of samples used for training and for testing the proposed system.. The samples images have bitmap (BMP) format with color depth 24 bit/pixel; and the size of each image is (1280x1024) pixels.

Two accuracy rates had been used for evaluating the system performance; they are (i) the allocation accuracy rate and (ii) the diagnosis accuracy rate. Allocation accuracy rate signifies the number of correct image blocks relative to the total number of blocks. On the other hand, the parameter "diagnosis accuracy rate" reflects the number of correct image samples relative to the total number of samples.

Table (1): The List of Number of Samples Used in the Feature Analysis & Testing Phases (when block size=150x150)

Class Name	Training		Testing	
	No. of Cases	No. of Samples	No. of Cases	No. of Samples
Normal	15	308	20	418
Benign	18	863	28	1368
Basal Cell Carcinoma	7	328	14	636
Squamous Cell Carcinoma	10	502	18	906
Total	50	2001	80	3328

A. Co-occurrence Features

Table (2) lists the attained recognition values when using co-occurrence features for different block sizes and when using one, two or three templates

Table (2): The Best Recognition Rates when Using Co-occurrence Matrix Features

SIZE OF BLOCKS	TOTAL NO. OF BLOCKS	NO. OF TEMPLATES	ALLOCATION ACCURACY RATE	DIAGNOSIS ACCURACY RATE
75X75	8093	1	80.77	88
		2	88.56	92
		3	88.98	92
100X100	4561	1	83.70	90
		2	91.54	94
		3	91.51	96
150X150	2001	1	85.69	92
		2	94.06	98
		3	92.67	96
200X200	1299	1	87.12	94
		2	93.97	96
		3	92.27	94
225X225	941	1	88.31	94
		2	93.45	96
		3	92.24	94

The best attained recognition rates (i.e., %94.06 for allocation accuracy rate and %98 for diagnosis accuracy rate) have been achieved when the size of blocks is set to (150x150). The result of testing all 80 samples, when using block size (150x150) and normalized city block distance, is (%85.70) for allocation accuracy rate, and (%91.25) for diagnosis accuracy rate. However, when retraining is done on the whole 80 cases, the result was (87.68) for allocation accuracy rate and (%92.5) for diagnosis accuracy rate.

B. RUN LENGTH FEATURES

Table (3) lists the attained recognition values when using run length features

Table (3): The Best Recognition Rates when Using Run Length Matrix Features

SIZE OF BLOCKS	TOTAL NO. OF BLOCKS	NO. OF USED TEMPLATES	ALLOCATION ACCURACY RATE(%)	DIAGNOSIS ACCURACY RATE(%)
75X75	8093	1	69.58	74
		2	68.98	72
		3	68.17	72
100X100	4561	1	72.26	78
		2	71.72	76
		3	69.26	74
150X150	2001	1	72.39	80
		2	67.88	74
		3	64.71	70
200X200	1299	1	72.52	82
		2	69.21	78
		3	63.48	70
225X225	941	1	73.30	84
		2	69.32	78
		3	62.99	70

The best attained recognition rates (i.e., 73.30% for allocation accuracy rate and 84% for diagnosis accuracy rate) have been achieved when the size of blocks is set to (225x225).

C. GLOBAL ROUGHNESS FEATURES

Table (4) lists the attained recognition values when using global roughness features.

Table (4): The Best Recognition Rates when Using Global Roughness Features

SIZE OF BLOCKS	TOTAL NO. OF BLOCKS	NO. OF TEMPLATES	ALLOCATION ACCURACY RATE (%)	DIAGNOSIS ACCURACY RATE (%)
75X75	8093	1	68.59	64
		2	76.30	78
		3	77.64	80
100X100	4561	1	65.96	62
		2	76.33	80
		3	78.25	84
150X150	2001	1	67.10	62
		2	77.29	80
		3	75.47	78
200X200	1299	1	67.26	64
		2	75.09	78
		3	77.38	80
225X225	941	1	72.00	70
		2	74.79	78
		3	77.77	82

The best attained recognition rates (i.e., 78.25% for allocation accuracy rate and 84% for diagnosis accuracy rate) have been achieved when the size of blocks is set to (225x225).

D. LOCAL ROUGHNESS FEATURES

Table (5) lists the attained recognition values when using local roughness features. The best attained recognition rates (i.e., 83.52% for allocation accuracy rate and 96% for diagnosis accuracy rate) are achieved when the size of blocks is set to (225x225).

Table (5): The Attained Recognition Rates when Using Local Roughness Features

SIZE OF BLOCKS	TOTAL NO. OF BLOCKS	NO. OF TEMPLATES	ALLOCATION ACCURACY RATE (%)	DIAGNOSIS ACCURACY RATE (%)
75X75	8093	1	73.94	86
		2	79.44	90
		3	80.39	92
100X100	4561	1	73.39	88
		2	80.41	90
		3	82.56	94
150X150	2001	1	77.43	88
		2	80.31	92
		3	81.47	92
200X200	1299	1	78.37	90
		2	79.63	92
		3	80.41	94
225X225	941	1	80.76	92
		2	83.21	94
		3	83.52	96

E. Combination of all Previous Texture Features

Table (6) lists the attained recognition values when combining the all previous texture features.

Table (6): The Recognition Rates when Using Combination of Different Texture Features

Size of Blocks	Total No. of Blocks	No. of Templates	Allocation Accuracy Rate (%)	Diagnosis Accuracy Rate (%)
75X75	8093	1	83.34	92
		2	88.71	94
		3	89.36	94
100X100	4561	1	86.39	92
		2	92.39	92
		3	92.42	94
150X150	2001	1	86.77	92
		2	94.22	98
		3	94.45	98
200X200	1299	1	89.54	94
		2	94.97	98
		3	94.44	96
225X225	941	1	90.91	94
		2	95.94	96
		3	96.10	96

The best attained recognition rates (i.e., 94.97% for allocation accuracy rate and 98% for diagnosis accuracy rate) are achieved when the size of blocks is set to (200x200). The results of testing all 80 samples, when using block size (200x200) and normalized city block distance was (%85.65) for allocation accuracy rate, and (%91.25) for diagnosis accuracy rate. However, with retraining the whole 80 cases, the result was improved to be (%89.92) for allocation accuracy rate and (%93.75) for diagnosis accuracy rate.

4. Conclusion

The objective of this paper is to design an automated system that diagnosis skin cancer using different texture features. The highest recognition rates reached by the proposed system was (%87.68) for allocation accuracy rate, and (%92.5) for diagnosis accuracy rate when using co-occurrence features, while when using combinations of different textural types of features the best recognition rates reached to (%89.92) for allocation accuracy rate, and (%93.75) for diagnosis accuracy rate .

References

[1] T.Y. Satheesha, D.S. Narayana, and M.N. Giriprasad, "Review on Early Detection of Melanoma in Situ", International Journal of Advanced Technology & Engineering Research (IJATER) National Conference on Emerging Trends in Technology (NCET-Tech), ISSN No: 2250-3536, Volume 2, Issue 4, July 2012.

[2] M.A. Sheha, M.S. Mabrouk, and A. Sharawy, "Automatic Detection of Melanoma Skin Cancer using Texture Analysis", International Journal of Computer Applications (0975 – 8887), Volume 42– No.20, March 2012.

[3] D.J. Gawkrodger, "Dermatology: An Illustrated Color text", 2002.

[4] S. Kia, S. Setayeshi, M. Shamsaei, M. Kia, "Computer-aided diagnosis (CAD) of the skin disease based on an intelligent classification of sonogram using neural network", Springer-Verlag, Neural Computing & Applications, 2012.

[5] C. Demir, and B. Yener, "Automated cancer diagnosis based on histopathological images: a systematic survey", Technical Report, Rensselaer Polytechnic Institute, Department of Computer Science, TR-05-09.

[6] R. Dobrescu, S. Mocanu, and D. Popescu, "Medical images classification for skin cancer diagnosis based on combined texture and fractal analysis", "Politehnica" University of Bucharest, Faculty of Control and Computers, 313 Splaiul Independentei, ISSN: 1109-9518, Issue 3, Volume 7, July 2010.

[7] M. Sadeghi, "Towards Prevention and Early Diagnosis of Skin Cancer: Computer-Aided analysis of Dermoscopy Images", PhD Dissertation, School of Computing Science Faculty of Applied Sciences, Iran, 2006.